ELSEVIER
Chemical Engineering Journal 142 (2008) 56–64
Chemical Engineering Journal
www.elsevier.com/locate/cej

Degradation of an azo dye Orange II using a gas phase dielectric barrier discharge reactor submerged in water

Young Sun Mok[a,*], Jin-O. Jo[a], J. Christopher Whitehead[b,**]

[a] *Department of Chemical Engineering, Cheju National University, Jeju 690-756, Republic of Korea*
[b] *School of Chemistry, The University of Manchester, Oxford Road, Manchester M13 9PL, UK*

Received 13 August 2007; received in revised form 9 November 2007; accepted 12 November 2007

Abstract

A dielectric barrier discharge (DBD) system employing wastewater as one of the electrodes was applied to the degradation of an azo dye, Orange II. The main advantage of this system is that reactive species like ozone and ultraviolet (UV) light produced by the DBD can be utilized for the treatment of wastewater. This system was able to remove the chromaticity and destroy the benzene and naphthalene rings in the dye molecule effectively. The results obtained under several conditions revealed that the UV emission from the DBD reactor could enhance the degradation of the dye, particularly in the presence of titanium oxide photocatalyst. The products resulting from the destruction of the rings in the dye molecule were found to be highly recalcitrant against further oxidation to smaller molecules. The change in the initial dye concentration showed that the reaction order was around 0.8 with respect to the dye concentration. The reduction in the concentration of total organic carbon was much more efficient with oxygen than with air.

Keywords: Dielectric barrier discharge; Ozone; Ultraviolet light; Wastewater; Dye

1. Introduction

The main merits of electrical discharge plasmas in environmental applications may be the in situ generation of strong oxidizing agents such as ozone and hydroxyl radicals, which are highly effective for removing contaminants from polluted gas or water [1–3]. In the area of water purification using electrical discharge plasmas, several types of pulsed corona discharge and dielectric barrier discharge (DBD) systems have been investigated [4–8]. These include pulsed corona discharge reactor with both electrodes submerged in water that creates plasma directly in aerated water, corona discharge reactor with one of the electrodes submerged in water and the other one placed above the surface of water, DBD reactor with one of the electrodes submerged in water and the other dielectric-covered electrode placed above the water that creates plasma in the gas phase between the dielectric material and the surface of water, and DBD reactor immersed in water. These systems have been applied to the abatement of various organic contaminants including phenol and its derivatives [7,9], polychlorinated biphenyl [10,11], organic dyes [12,13], aniline [14], anthraquinone [15], etc.

The most abundant oxidizing species produced by the above electrical discharge plasmas with the addition of air or oxygen is ozone that is formed in the gas phase, although small amounts of other species such as hydrogen peroxide, hydroxyl radicals, and hydroperoxyl radicals are also produced in the water phase. Therefore, to efficiently utilize the ozone for removing water contaminants, it is very important to increase the interfacial area between the water phase and the gas phase as much as possible. In this context, the corona discharge or DBD above the surface of water having a very limited area available for chemical reactions may not be suitable for practical applications. One simple and convenient method to increase the interfacial area is to disperse the gas energized in the DBD reactor in the water phase in the form of fine bubbles. Taking a

---

* Corresponding author. Tel.: +82 64 754 3680; fax: +82 64 755 3670.
** Corresponding author. Tel.: +44 161 275 4692; fax: +44 161 275 4598.
E-mail addresses: smokie@cheju.ac.kr (Y.S. Mok), j.c.whitehead@manchester.ac.uk (J.C. Whitehead).

1385-8947/$ – see front matter © 2007 Elsevier B.V. All rights reserved.
doi:10.1016/j.cej.2007.11.012

broad view, ozone can oxidize contaminants in water in two ways [16,17]. Firstly, gaseous ozone and dissolved ozone can directly react with the contaminants at the gas–liquid interface and in the bulk phase, respectively. Besides this direct oxidation of the contaminants, ozone dissolved in water decomposes into hydroxyl radicals having high oxidation potential, which react quickly with the contaminants. As well as producing chemically reactive species, it has been reported that the electrical discharge plasmas bring about physical processes like emission of ultraviolet (UV) and visible photons [18,19]. Thus, if photocatalysis is incorporated into an electrical discharge system, the performance of water treatment will be enhanced. Mok et al. [8] showed that the UV photons emitted from the DBD reactor could activate the photocatalyst to degrade the organic contaminant in water, and Li et al. [12] observed that the decoloration efficiency for a dyeing wastewater significantly increased by adding titanium oxide particles into the reactor of a pulsed discharge with a needle-to-plate electrode configuration.

In this study, we investigated the application of a DBD reactor submerged in water to the degradation of an organic contaminant. An azo dye, Orange II, was selected as the model organic contaminant, which was dissolved in distilled water to form a synthetic wastewater. As will be described below, the DBD reactor of the present investigation acted not only as a means to generate reactive species but also as an UV/visible lamp. The reactor consisted of a quartz tube and a concentric copper electrode to where high voltage is applied. The influence of the reactive species (mainly ozone) produced in the DBD reactor and DBD-induced photocatalysis on the degradation of the organic contaminant was examined, and several byproducts were analyzed. The degradation of the organic contaminant was assessed by UV/visible absorbance and measurement of the concentration of total organic carbon (TOC).

2. Experimental

The schematic diagram of the experimental setup is shown in Fig. 1, where the cross-sectional view is also given. The reactor vessel containing wastewater had 90 mm inner diameter and 200 mm length. The DBD reactor immersed in the wastewater comprised a quartz tube with its respective inner and outer diameters of 22 and 25 mm, and a 9 mm copper rod. An AC high voltage of 13.4–23.3 kV (RMS value) was applied to the copper electrode while the wastewater was connected to the ground electrode. Note that the wastewater is electrically conductive and it elongates the ground electrode up to the outer surface of the quartz tube. The electrical discharge occurs in the space between the copper electrode and the inner surface of the quartz tube, where ozone and UV are produced. The gas flowing through this space can be air or oxygen. The voltage applied to the copper electrode was measured by a 1000:1 high voltage probe (PVM-4, North Star Research, Corp.) and a digital oscilloscope (TDS 3032, Tektronix). The discharge power of the DBD reactor was measured by the so-called Lissajous figure [20].

The synthetic wastewater was prepared with distilled water and an azo dye Orange II as the model organic compound. Orange II (sodium salt form, $C_{16}H_{11}N_2NaO_4S$, formula weight: 350.32) was purchased from Sigma–Aldrich Co. The molecular structure of Orange II is given in Fig. 2. The volume of the wastewater and the typical concentration of the organic contaminant were 500 mL and 25 mg/L (0.071 mM), respectively. The initial concentration of the organic contaminant was varied from 10–100 mg/L (0.029–0.285 mM). The aqueous Orange II

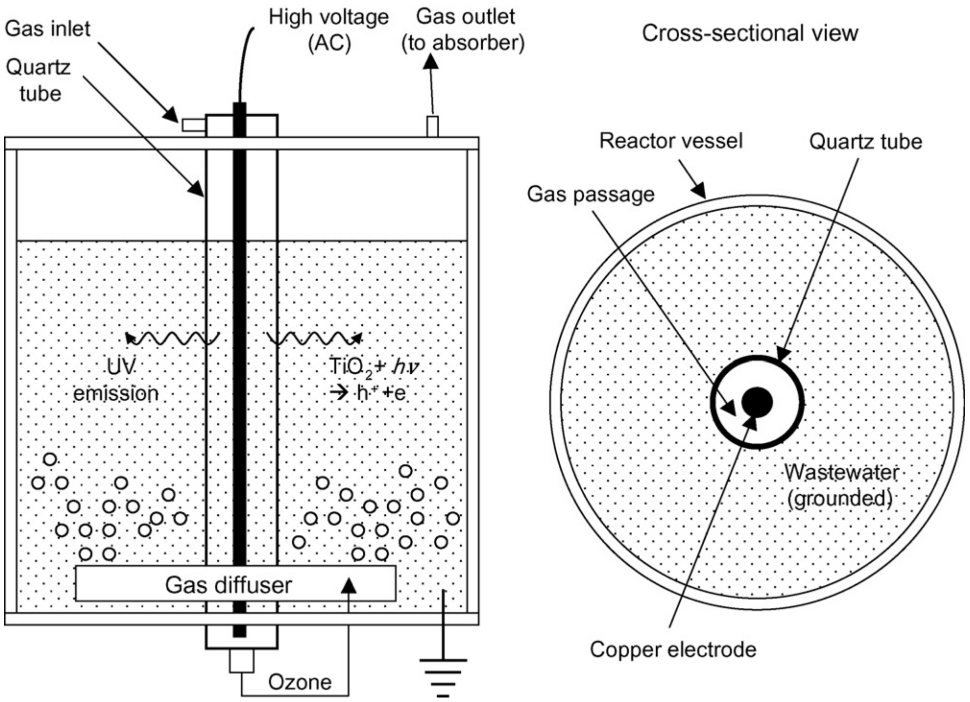

Fig. 1. Schematic diagram of the experimental apparatus.

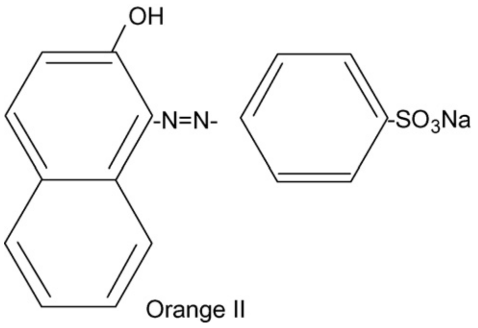

Fig. 2. Molecular structure of azo dye Orange II.

solution was slightly acidic with a pH value of 5.3. So as to utilize the UV/visible light emitted from the DBD reactor for the degradation of the organic contaminant, powdery photocatalyst was added to the wastewater The photocatalyst employed was commercial titanium dioxide powder (Degussa P25) with a BET surface area of 50 m^2/g and an average particle size of 30 nm. The concentration of the titanium dioxide powder was changed from 0.6 to 1.0 g/L. It is well known that titanium dioxide can adsorb some amount of the dye. Thus, in the cases that the photocatalyst was used, the concentration of the dye after adsorption saturation was adopted as the initial concentration. In the presence of the photocatalyst and UV light, the addition of hydrogen peroxide to the wastewater enhances the production of hydroxyl radicals. The concentration of hydrogen peroxide was varied up to 0.16 mol/L. The gas fed to the DBD reactor was typically dry air whose flow rate was adjusted to 6 L/min. In some experiments, oxygen was used as the working gas.

The experiments for the degradation of the organic contaminant were conducted by continuously transferring the gas previously energized in the DBD reactor to the synthetic wastewater at the bottom of the reactor vessel through a porous gas diffuser. As understood in Fig. 1, the concentration of ozone emitted from the DBD reactor corresponds to that at the inlet of the reactor vessel. The depth of the wastewater in the reactor vessel was about 95 mm without transferring the gas, and it slightly increased due to the gas bubbles when the gas was transferred. Since the wastewater itself acted as the ground electrode, the depth of the wastewater defined the discharge region. Samples were taken from the reactor vessel at appropriate time intervals, and analyzed by an UV/visible spectrophotometer (HP8453, Hewlett Packard) at 484 and 310 nm. The absorbance at 484 nm is related to the chromaticity while that at 310 nm is related to the vibration of the naphthalene ring in the Orange II molecule [21,22]. A TOC analyzer (TOC-5000A, Shimadzu) was also used to assess the degradation of the organic contaminant. The UV irradiation intensity was measured with a radiometer (VLX-365, Vilber Lourmat), which covers the UVA band. The concentration of ozone produced in the DBD reactor was analyzed by an UV/visible spectrophotometer (UV-2500, Labomed, Inc.) at 260 nm.

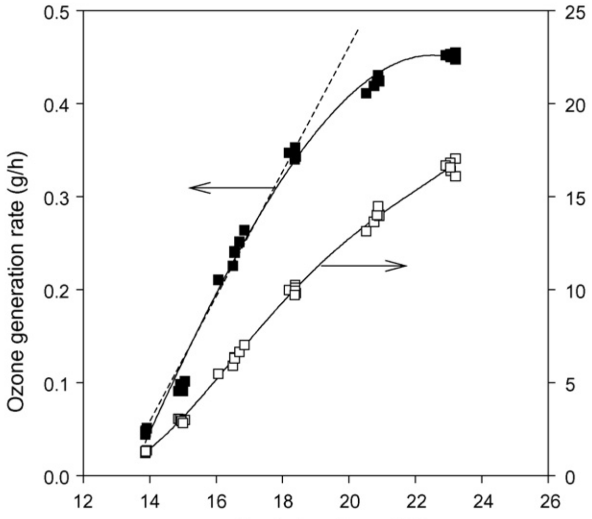

Fig. 3. Effect of the applied voltage (RMS) on the ozone generation rate and the discharge power.

3. Results and discussion

3.1. Ozone generation rate

Fig. 3 shows the ozone generation rate and the discharge power as a function of the voltage applied to the DBD reactor. The voltage was changed from 13.4 to 23.3 kV (RMS value) to increase the discharge power, thereby increasing the ozone generation rate. The concentration of ozone was measured in the gas phase. It was observed that the ozone generation rate increased almost linearly with the increase in the voltage up to about 18.5 kV and then slowed down as the voltage was increased further. The increase in the voltage generates more ozone as a result of the increases in the discharge power and the electric field strength, but as the concentration of ozone increases, the rate of the decomposition of the generated ozone also increases. This is why the ozone generation rate slowed down at voltages higher than 18.5 kV. When the voltage was 18.5 and 23.3 kV, the corresponding discharge power was 10.0 and 16.8 W, respectively. At these discharge powers, the ozone generation rates were about 0.35 and 0.45 g/h, which correspond to energy yields of 0.035 and 0.027 g/Wh.

3.2. Degradation of Orange II by the DBD

Fig. 4 shows the temporal variations of the UV/visible absorbance at 484 and 310 nm for the samples taken from the wastewater. The results in Fig. 4 were obtained at three different experimental conditions, namely, (1) with only ozone, (2) with ozone plus UV (basic condition), and (3) with ozone plus UV plus titanium oxide at a discharge power 16.8 W. The reactor system shown in Fig. 1 simultaneously ozonizes and irradiates the wastewater. So as to exclude the effect of the UV emitted from the DBD reactor on the degradation (Case 1), two reactor systems that were exactly the same were used, i.e., ozone produced in one of the reactor systems was transferred to the other one, thereby evaluating exclusively the effect of ozone on the degradation. As mentioned above, ozone can degrade the contaminant

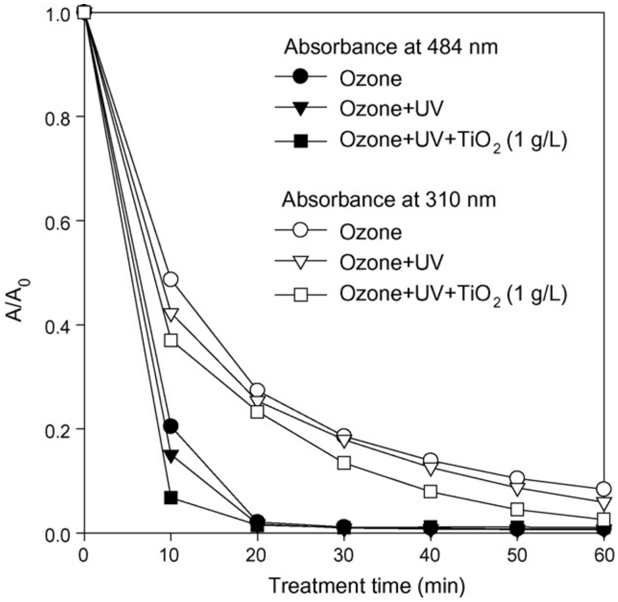

Fig. 4. Temporal variations of the absorbance at 484 and 310 nm for three degradation conditions.

by either direct oxidation or forming hydroxyl radicals:

- direct oxidation

$$O_3 + \text{organic} \rightarrow \text{products} \quad (1)$$

- formation of OH

$$O_3 \rightarrow O + O_2 \quad (2)$$

$$O + H_2O \rightarrow 2OH^\bullet \quad (3)$$

$$OH^- + O_3 \rightarrow O_2{}^- + HO_2 \quad (4)$$

$$O_2{}^- + O_3 + H^+ \rightarrow O_2 + HO_3 \quad (5)$$

$$HO_3 \rightarrow OH^\bullet + O_2 \quad (6)$$

$$OH^\bullet + \text{organic} \rightarrow \text{products} \quad (7)$$

As can be seen in Fig. 4, ozone had a great influence on the degradation of the dye. With only ozone (Case 1), the chromaticity (the normalized absorbance at 484 nm) almost disappeared within 20 min, and the normalized absorbance at 310 nm decreased by about 90% in 60 min, implying that most of the naphthalene rings in the dye molecules were destroyed [21]. When UV irradiation was added (Case 2), the normalized UV/visible absorbance at both 310 and 484 nm decreased slightly faster than Case 1 did. This result may be attributed to the decomposition of ozone by the UV photons [23]:

$$O_3 + h\nu \rightarrow O + O_2 \quad (8)$$

The oxygen atom produced reacts with water to form hydroxyl radicals as in reaction (3). The hydroxyl radical has an oxidation potential of 2.80 V, which is greater than 2.07 V for ozone [1]. Thus, the decomposition of ozone into an oxygen atom, eventually yielding more hydroxyl radicals, can enhance the degradation. The electrical discharge with air or nitrogen emits UV light mainly in the UVA band, although weak emission peaks of shorter wavelengths in the UVB band also appear [18,19]. It has been reported that the photodissociation of ozone occurs fast at wavelengths below 310 nm [24], but according to Wu et al. [25] who investigated the degradation of an azo dye Amaranth using an ozonation system combined with a 365 nm UV lamp, it is thought that the photons with longer wavelengths can also promote the decomposition of ozone. From several sets of comparative experiments, they found that the degradation of the dye by ozone in the presence of the 365 nm UV lamp was much faster than that with only ozone. In Fig. 4, the degradation of Orange II by ozone was not significantly enhanced in the presence of the UV irradiation, which is probably due to the fact that the rate of reaction between the dye and ozone was so fast as to obscure the UV irradiation effect. The other reason may be because the UV irradiation intensity of the DBD reactor was relatively lower than those of UV lamps commonly adopted in UV/O_3 systems. Case 3 mentioned above is for evaluating the combined effect of the DBD-induced photocatalysis and ozonation. As is well known, the titanium oxide photocatalyst absorbs the UV photons to produce hydroxyl radicals as follows [26–28]:

$$TiO_2 + h\nu \rightarrow e^- + h^+ \quad (9)$$

$$h^+ + H_2O \rightarrow H^+ + OH^\bullet \quad (10)$$

where e^- and h^+ are the electron in the conduction band and the electron vacancy in the valence band, respectively. Since the band-gap energy of anatase-form titanium oxide is approximately 3.2 eV, tantamount to the energy of 391 nm photons, the UV light emitted from the DBD reactor is strong enough to activate it. As expected, Case 3 comprising ozone, UV and photocatalyst was more effective in the degradation than only ozone or ozone plus UV, because additional hydroxyl radicals were formed by the photocatalyst. In Case 3, the chromaticity removal in 10 min was more than 90%, and the absorbance at 310 nm corresponding to the vibration of the naphthalene ring in the dye molecule decreased to nearly zero in 60 min. To summarize the results in Fig. 4, the rate of the degradation was in the order of Case 3, Case 2 and Case 1 from high to low.

In the above experiments, the working gas was dry air, which produces nitrogen oxides as well as ozone. At a discharge power 16.8 W, about 35 ppm of NO_2 was formed in the DBD reactor, though NO was not observed. When NO_2 is dissolved in water, it is converted into nitric and nitrous acids that decrease the pH value and increase the solution conductivity. For Case 2 as an example, the solution conductivity largely increased with the treatment time from 60 μS/cm at 0 min to 378 μS/cm at 60 min, and the pH value from 5.3 to 3.58. But, neither the discharge power nor the rate of ozone generation was affected by the solution conductivity in this range. This result can be explained as follows. Although the electric discharge (DBD) makes the working gas slightly conductive, the electrical resistance of the gas is much higher than that of the water, i.e., that of the gas dominates the overall resistance. The degradation products like organic acids can also change the pH value and the solution conductivity, but it is believed that the dissolution of NO_2 forming strong acids has more significant effect.

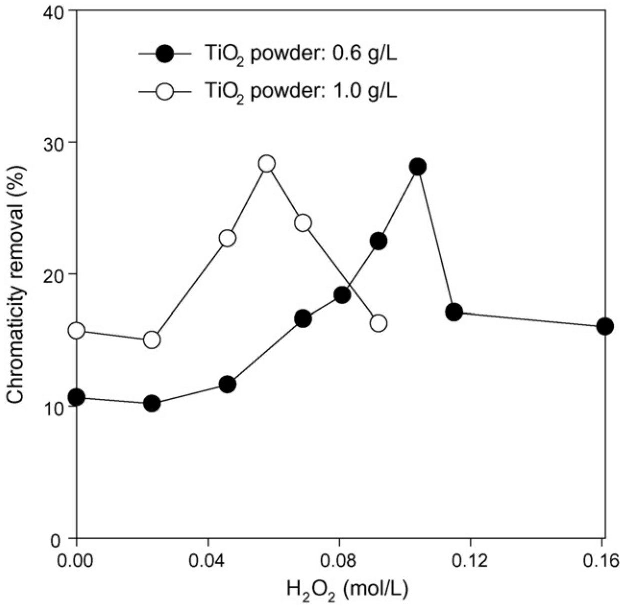

Fig. 5. Chromaticity removal efficiency obtained with only DBD-induced photocatalysis.

The effect of the photocatalysis alone in the absence of ozone was also evaluated. Fig. 5 shows the chromaticity removal efficiency obtained with only DBD-induced photocatalysis. The chromaticity removal efficiency was defined as the percentage of the decrease in the absorbance at 484 nm. For this experiment, ozone produced in the DBD reactor was not transferred to the wastewater. Instead, dry air of 6 L/min was injected into the wastewater through the above mentioned porous gas diffuser to mix the photocatalyst powder and the wastewater. The discharge power was adjusted to 16.8 W, and at this discharge power the UV intensity was 0.08 mW/cm^2. The content of titanium oxide powder added to the wastewater was 0.6 or 1.0 g/L. The addition of hydrogen peroxide often increases the rate of the degradation significantly. In the presence of hydrogen peroxide, electrons and holes as a result of reaction (9) give rise to following reactions [26,27]:

$$e^- + H_2O_2 \rightarrow OH^\bullet + OH^- \qquad (11)$$

$$h^+ + H_2O_2 \rightarrow H^+ + HO_2 \qquad (12)$$

$$HO_2 + HO_2 \rightarrow H_2O_2 + O_2 \qquad (13)$$

The hydroxyl radical formed by reaction (11) has much higher oxidation potential than hydrogen peroxide. As can be seen in Fig. 5, the increase in the concentration of hydrogen peroxide up to a certain value increased the chromaticity removal efficiency, but further increase brought about a contrary effect. This result is because additional hydrogen peroxide functions as a scavenger of the highly reactive hydroxyl radical to form much less reactive hydroperoxyl radical whose oxidation potential is 1.70 V [29]:

$$OH^\bullet + H_2O_2 \rightarrow H_2O + HO_2 \qquad (14)$$

The concentration of hydrogen peroxide showing maximum chromaticity removal efficiency depended on the content of titanium oxide powder. When the content of titanium oxide powder was 0.6 and 1.0 g/L, appropriate hydrogen peroxide concentration was found to be around 58 and 100 mM, respectively. As presented in Fig. 5, the rate of the photocatalytic degradation of Orange II was found to be slow, compared to that in the presence of ozone. When the pH of the wastewater was changed to acidic region (pH 4.0), the photocatalytic degradation rate was slightly enhanced, but still much slower than that in the presence of ozone. In our previous study, the DBD-induced photocatalytic degradation of an azo dye Acid Red 4 having a molecular structure similar to Orange II was investigated, and it was found that Acid Red 4 was easily degraded by the photocatalysis caused by the DBD [8]. Why Orange II was not easily degraded by the DBD-induced photocatalysis despite the similar molecular structure to Acid Red 4 is unclear. One plausible reason for this may be the difference in the UV/visible absorption spectrum. At an identical concentration, it was observed that Orange II absorbed more strongly in both the UV and visible wavelength range, resulting in the reduction of the amount of photons to be used for the activation of the photocatalyst.

3.3. Degradation products

Fig. 6 shows the UV/visible spectra of the samples taken from the wastewater after being treated for 60 min at three different conditions mentioned in Fig. 4. These spectra showing only one peak are much different from the spectrum of the original Orange II solution. In all three cases, maximum absorbance occurred at around 210 nm, which is attributed to the presence of the byproducts produced from the dye. In this study, the byproducts were not fully identified, but these spectra indicate that most of the benzene and naphthalene rings existing in the original dye molecules were destroyed. Benzene exhibits an absorption band at 260 nm that is linked with the π-system of its ring structure,

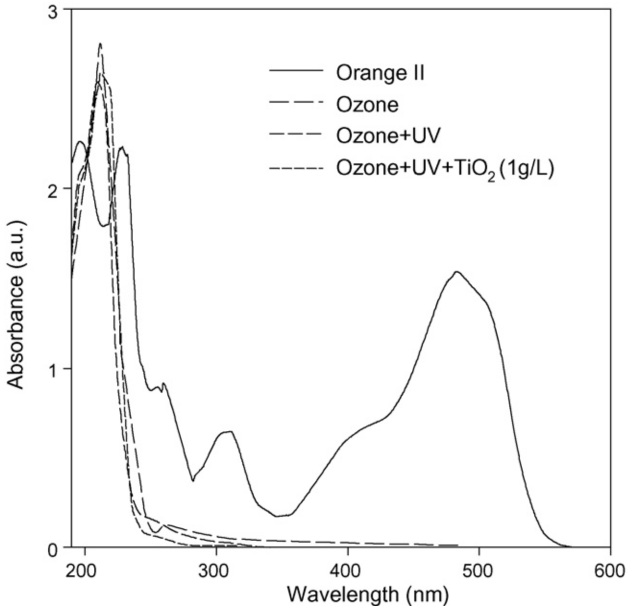

Fig. 6. UV/visible spectra for three degradation conditions (treatment time: 60 min).

although the band shifts to larger wavelength when substituents are present [30]. The spectra presented in Fig. 6 have very low absorbance at wavelengths larger than 260 nm, which reveals that very little amount of aromatic species remained.

According to the degradation pathway proposed by Zhao et al. [31], the main byproducts formed by the ozonation of azo dye are organic acids, aldehydes, ketones, and carbon dioxide. Meanwhile, Demirev and Nenov [32] suggested that the eventual degradation products of azo dye in the ozonation system would be acetic, formic and oxalic acids. In this study, a high performance liquid chromatograph (HPLC) analysis was made for such small organic acids as acetic, formic and oxalic acids. The wastewater was treated by Case 2 (ozone plus UV) mentioned in Fig. 4, and samples were taken at every 10 min for 60 min. No such acids were detected till 60 min, and from the sample taken at 60 min, 1.8 mg/L of oxalic acid and trace amounts of acetic and formic acids were detected. This oxalic acid concentration is very low, compared to the initial concentration of the dye 25 mg/L. As described above, the chromaticity of the wastewater disappeared fast and the ring structures in the dye molecule were effectively destroyed, but the fact that only a small amount of oxalic acid was formed implies that the products resulting from the destruction of the ring structures are highly recalcitrant against further oxidation to oxalic, acetic and formic acids. The vapor pressure of oxalic acid at 20 °C is less than 1.3×10^{-4} kPa, but acetic acid and formic acid whose vapor pressures are 3.3 and 5.4 kPa at the same temperature are volatile enough to be released into the gas phase. To measure the amount of the organic acids if they were released into the gas phase, the gas coming out of the reactor vessel was passed through an absorber containing 500 mL of 0.01 M aqueous NaOH solution for 60 min, and the concentration of organic carbon in the absorbing solution was analyzed. The concentration of total organic carbon in the NaOH solution was found to be negligible, indicating that only small amount of volatile organic byproducts were formed from the dye.

3.4. Ozone consumption

Fig. 7 shows the mass ratio of the ozone reacted to the dye degraded as a function of the discharge power, where the mass ratio of the ozone fed to the dye degraded is also presented. As presented in Fig. 3, the increase in the discharge power increases the ozone generation rate. The amount of ozone reacted was estimated by monitoring its concentration difference between the inlet and outlet of the reactor vessel:

$$\text{Ozone reacted} = Q\int_0^t ([\mathrm{O_3}]_{\mathrm{in}} - [\mathrm{O_3}]_{\mathrm{out}})\,\mathrm{d}t' \tag{15}$$

where Q is the gas flow rate, $[\mathrm{O_3}]_{\mathrm{in}}$ and $[\mathrm{O_3}]_{\mathrm{out}}$ are the concentrations of ozone at the inlet and outlet of the reactor vessel, and t is the treatment time. The amount of ozone fed and the amount of the dye degraded were calculated as follows:

$$\text{Ozone fed} = Q[\mathrm{O_3}]_{\mathrm{in}}t \tag{16}$$

$$\text{Dye degraded} = V(C_0 - C_{\mathrm{f}}) \tag{17}$$

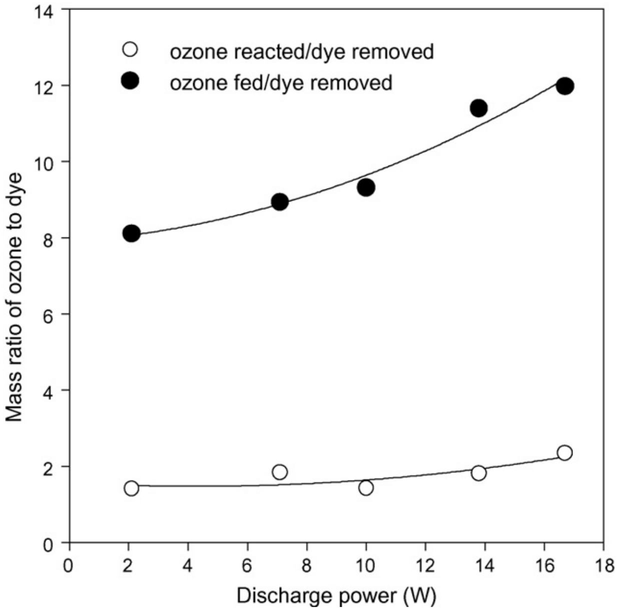

Fig. 7. The amount of ozone required for degrading Orange II.

where V is the volume of the wastewater, and C_0 and C_{f} are the initial and final concentration of the dye. The initial concentration of the dye in the wastewater was 25 mg/L. For this experiment, the amount of ozone fed relative to that of the dye was varied from 8 to 12 on the basis of mass by changing the discharge power. As can be seen in Fig. 7, the amount of the ozone reacted was on average about 1.8 times (13 times on molar basis) more than that of the dye degraded. The reason that more ozone is required than stoichiometric value is because the dye molecule has many reactive sites and its degradation includes several consecutive oxidation steps.

3.5. Effect of the initial dye concentration

Most of studies on the degradation of dye assumed that the degradation by ozone was a first-order reaction with respect to its concentration [23,32,33]. However, since the dye has several reactive sites, it is not reasonable to assume that the reaction between the dye and ozone is first order. The effect of the initial concentration on the degradation was examined in the range of 10–100 mg/L at a discharge power of 16.8 W. As shown in Fig. 8, the degradation of the dye was dependent on the initial concentration. If the reaction was first order, all data should be on the same curve regardless of the initial concentration. The rate of the reaction between the dye and ozone can generally be written as

$$-\frac{\mathrm{d}C}{\mathrm{d}t} = k'[\mathrm{O_3}]^a C^b \tag{18}$$

where k' is the rate constant, and a and b are the reaction orders. In this study, ozone was fed in excess, and thus its concentration can be treated as a constant [34]. In this case, Eq. (18) can be rewritten as below

$$-\frac{\mathrm{d}C}{\mathrm{d}t} = kC^b \tag{19}$$

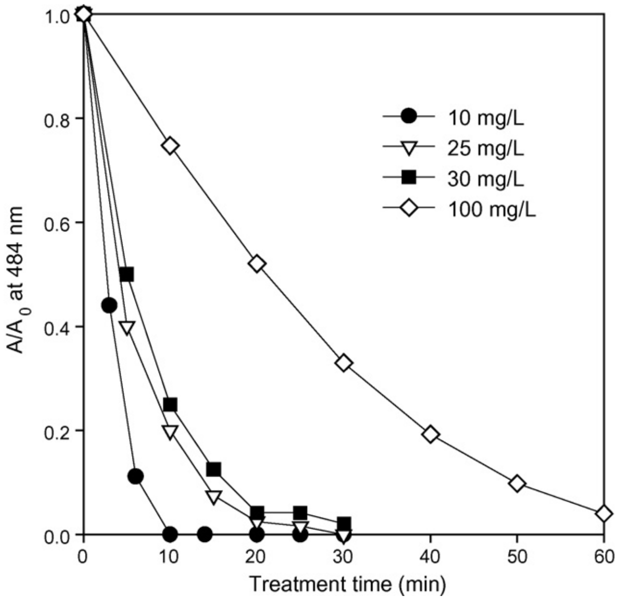

Fig. 8. Effect of the initial concentration of the dye on the chromaticity removal.

where k is $k'[O_3]^a$. Since the concentration of ozone generated is a function of the discharge power, the apparent rate constant k also depends on it. Eq. (19) can be rewritten to give

$$\ln\left(-\frac{dC}{dt}\right) = \ln k + b \ln C \tag{20}$$

$$\ln \frac{C_t - C_{t+\Delta t}}{\Delta t} = \ln k + b \ln \frac{C_{t+\Delta t} + C_t}{2} \tag{21}$$

The data in Fig. 8 were recomposed in terms of Eq. (21), which summarized in Fig. 9. The slope of each straight line corresponds to the reaction order b. The slope was found to be around 0.8 (0.775 at 10 mg/L, 0.789 at 25 mg/L, 0.791 at 30 mg/L), regardless of the initial concentration when it was in the range of 10–30 mg/L. On the other hand, the slope decreased to 0.6 when the initial concentration increased to 100 mg/L. When simplifying Eq. (18) to (19), ozone was assumed to be in excess. But, for the initial dye concentration of 100 mg/L, this assumption does not seem to be valid. Thus, it is reasonable to consider the reaction order as 0.8 with respect to the concentration of the dye.

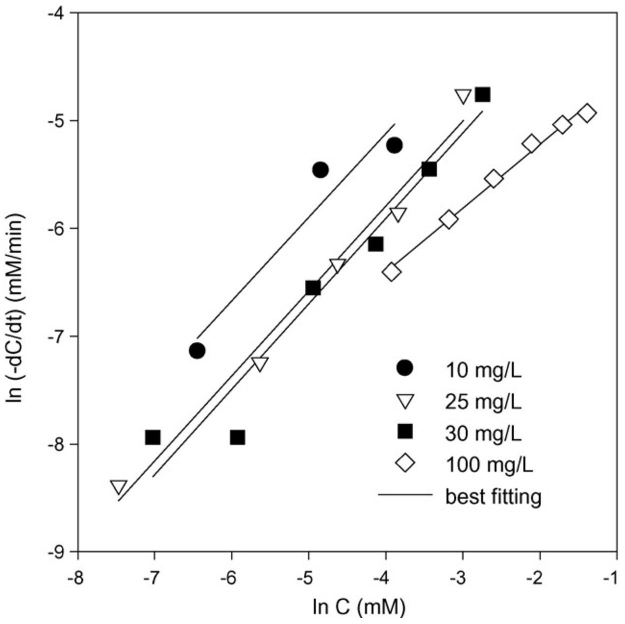

Fig. 9. Relation of the time derivative with the concentration.

3.6. Effect of the working gas

The most important role of the DBD in the degradation of the dye is the generation of ozone, which is deeply related to the content of oxygen in the working gas. Fig. 10(a and b) shows the effect of the type of working gas on the UV/visible absorbance

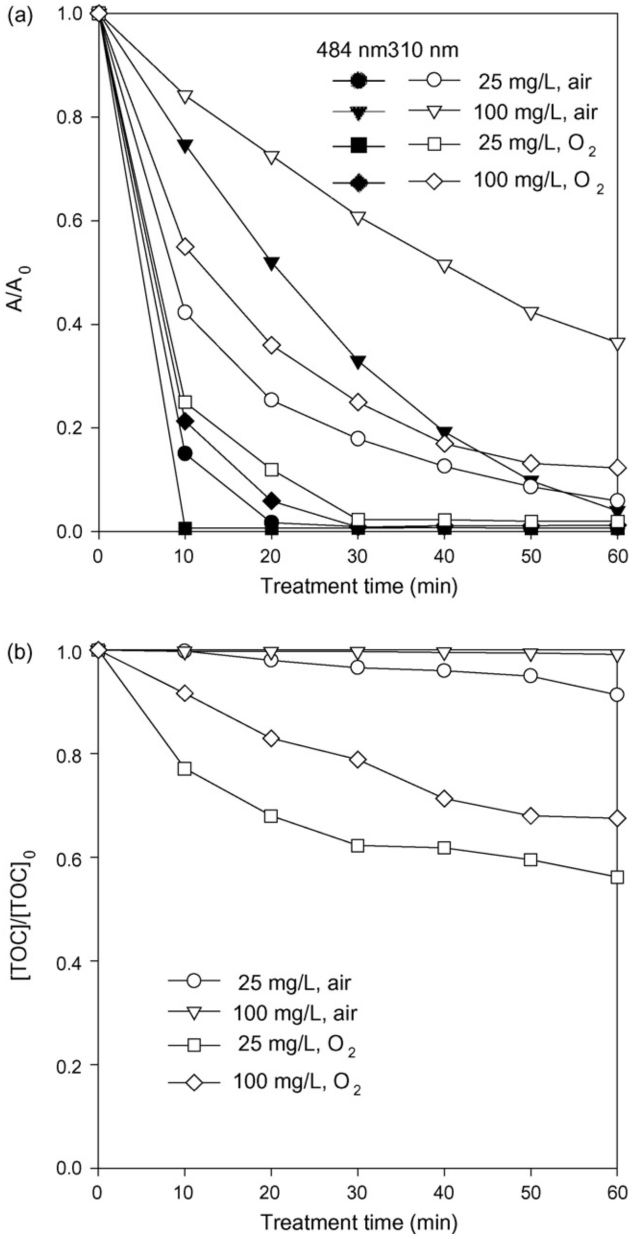

Fig. 10. Effect of the working gas on the absorbance at 484 and 310 nm (a), and on the concentration of total organic carbon (b).

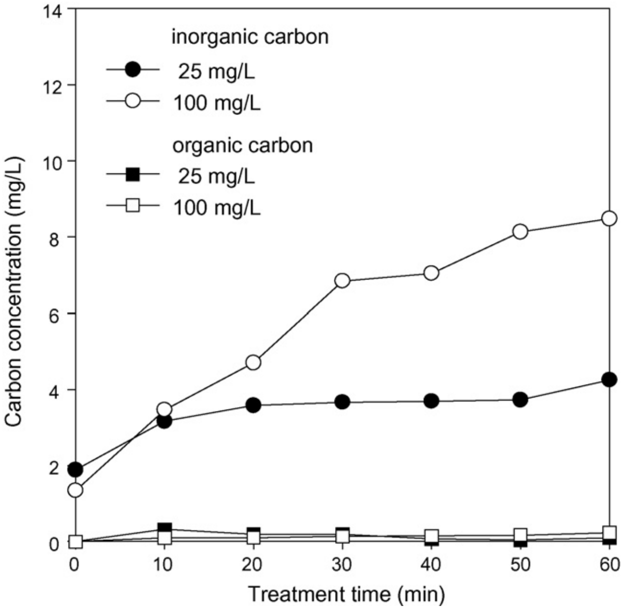

Fig. 11. Carbon concentration in the sodium hydroxide absorbing solution.

and the TOC concentration. When pure oxygen was used as the working gas, the UV/visible absorbance at both 484 and 310 nm decreased much faster than in the case of using air. This result is definitely due to the increase in the concentration of ozone when using oxygen. With oxygen, the time required for the removal of chromaticity (absorbance at 484 nm) was shortened a lot, and the absorbance at 310 nm was much lowered, compared to the case with air. In addition to the UV/visible absorbance, another notable difference between oxygen and air relates to the concentration of TOC. As can be seen, little amount of the TOC was removed with air while 44 and 32% of TOC was removed with oxygen when the initial concentration was 25 and 100 mg/L, respectively. This reduction in the concentration of TOC with oxygen indicates that some inorganic or volatile organic compounds formed were released into the gas phase. To examine whether volatile organic compounds were formed from the dye and released, the gas from the reactor vessel was passed through an absorber that contained 500 mL of 0.01 M aqueous NaOH solution, and the concentration of carbon in the NaOH solution was analyzed. Fig. 11 shows the concentration of organic and inorganic carbon in the absorbing solution when the initial concentration of the dye was 25 and 100 mg/L. Since the working gas was pure oxygen in this case, all the organic and inorganic carbons in the absorbing solution were originated from the dye. As can be seen, the concentration of inorganic carbon, i.e., carbon dioxide, tended to increase with the treatment time. On the other hand, the concentration of organic carbon in the absorbing solution was almost negligible, revealing that the major byproducts are not small volatile organic acids.

4. Conclusions

The dielectric barrier discharge reactor in water capable of ozonizing and UV-irradiating concurrently was very effective in degrading the organic contaminant, Orange II. The chromaticity of the synthetic wastewater rapidly disappeared, and the ring structures in the dye molecule were effectively destroyed. But, the results obtained with a high performance liquid chromatograph and a total organic carbon (TOC) analyzer indicated that the products resulting from the destruction of the rings in the dye molecule were quite refractory to further oxidation. Compared to the case of ozone alone, better degradation results were obtained in the presence of UV. The amount of ozone consumed was about 1.8 times that of the dye degraded on mass basis. The reaction order was estimated to be around 0.8 with respect to the dye concentration. The type of working gas had a great influence on the concentration of TOC. For instance, when the initial dye concentration was 25 mg/L, the reduction in TOC was 9 and 44% with air and oxygen, respectively. With this system, the dye was not completely mineralized to carbon dioxide. Nevertheless, considering that the chromaticity removal has been the main goal in the textile industry, the present system may be promising.

Acknowledgements

This work was supported by the Research Abroad Grant from the Chuongbong Academic Research Fund of the Cheju National University in 2006, and by the UK Engineering and Physical Sciences Research Council.

References

[1] B. Sun, M. Sato, J.S. Clements, Optical study of active species produced by a pulsed streamer corona discharge in water, J. Electrostat. 39 (1997) 189–202.

[2] H.H. Kim, Nonthermal plasma processing for air-pollution control: a historical review, current issues, and future prospects, Plasma Proc. Polym. 1 (2004) 91–110.

[3] P. Lukes, T. Appleton, B.R. Locke, Hydrogen peroxide and ozone formation in hybrid gas–liquid electrical discharge reactors, IEEE Trans. Ind. Appl. 40 (2004) 60–67.

[4] M.A. Malik, A. Ghaffar, S.A. Malik, Water purification by electrical discharges, Plasma Sour. Sci. Technol. 10 (2001) 82–91.

[5] Y.-K. Kim, S.A. Kim, S.B. Lee, J.-K. Kim, D.-W. Kang, Decomposition of ethylenediaminetetraacetic acid using He-Ar-O_2 dielectric barrier discharge, Plasma Proc. Polym. 2 (2005) 252–255.

[6] B.R. Locke, M. Sato, P. Sunka, M.R. Hoffmann, J.S. Chang, Electrohydraulic discharge and non-thermal plasma for water treatment, Ind. Eng. Chem. Res. 45 (2006) 882–905.

[7] M. Dors, J. Mizeraczyk, Y.S. Mok, Phenol oxidation in aqueous solution by gas phase corona discharge, J. Adv. Oxid. Technol. 9 (2006) 139–143.

[8] Y.S. Mok, J.-O. Jo, C. Woo, Gaseous electrical discharge-induced degradation of organic compound in wastewater: UV irradiation and ozonation effect, J. Adv. Oxid. Technol. 10 (2007) 439–446.

[9] A.G. Bubnov, E.Y. Burova, V.I. Grinevich, V.V. Rybkin, J.-K. Kim, H.-S. Choi, Plasma-catalytic decomposition of phenols in atmospheric pressure dielectric barrier discharge, Plasma Chem. Plasma Proc. 26 (2006) 19–30.

[10] M. Sahni, W.C. Finney, B.R. Locke, Degradation of aqueous phase polychlorinated biphenyls (PCB) using pulsed corona discharges, J. Adv. Oxid. Technol. 8 (2005) 105–111.

[11] Y.Z. Wen, X.Z. Jiang, Pulsed corona discharge-induced reactions of acetophenone in water, Plasma Chem. Plasma Proc. 21 (2001) 345–354.

[12] J. Li, Z. Zhou, H. Wang, G. Li, Y. Wu, Research on decoloration of dye wastewater by combination of pulsed discharge plasma and TiO_2 nanoparticles, Desalination 212 (2007) 123–128.

[13] Y.S. Mok, J.-O. Jo, Degradation of a textile azo dye by pulsed arc discharge to the surface of wastewater, Korean J. Chem. Eng. 24 (2007) 607–611.

[14] M. Tezuka, M. Iwasaki, Plasma-induced degradation of aniline in aqueous solution, Thin Solid Films 386 (2001) 204–207.

[15] A.L. Bozic, N. Koprivanac, P. Sunka, M. Clupek, V. Babicky, Organic synthetic dye degradation by modified pinhole discharge, Czech. J. Phys. 54 (2004) C958–C963.

[16] E.J. Rosenfeldt, K.G. Linden, S. Canonica, U. von Gunten, Comparison of the efficiency of OH radical formation during ozonation and the advanced oxidation processes O_3/H_2O_2 and UV/H_2O_2, Water Res. 40 (2006) 3695–3704.

[17] T.A. Kurniawan, W. Lo, G.Y.S. Chan, Radicals-catalyzed oxidation reactions for degradation of recalcitrant compounds from landfill leachate, Chem. Eng. J. 125 (2006) 35–57.

[18] Y. Kim, S.H. Hong, M.S. Cha, Y.H. Song, S.J. Kim, Measurements of electron energy by emission spectroscopy in pulsed corona and dielectric barrier discharges, J. Adv. Oxid. Technol. 6 (2003) 17–22.

[19] R. Zhang, L. Wang, C. Zhang, Y. Nie, Y. Wu, Z. Guan, Spectroscopic investigation of the bipolar pulsed discharge in water–air mixture, IEEE Trans. Plasma Sci. 34 (2006) 1033–1037.

[20] L.A. Rosocha, Nonthermal plasma applications to the environment: gaseous electronics and power conditioning, IEEE Trans. Plasma Sci. 33 (2005) 129–137.

[21] W. Feng, D. Nansheng, H. Helin, Degradation mechanism of azo dye C. I. Reactive Red 2 by iron powder reduction and photooxidation in aqueous solutions, Chemosphere 41 (2000) 1233–1238.

[22] M. Stylidi, D.I. Kondarides, X.E. Verykios, Visible light-induced photocatalytic degradation of Acid Orange 7 in aqueous TiO_2 suspensions, Appl. Catal. B: Environ. 47 (2004) 189–201.

[23] G. Tezcanli-Güyer, N.H. Ince, Individual and combined effects of ultrasound, ozone and UV irradiation: a case study with textile dyes, Ultrasonics 42 (2004) 603–609.

[24] S.M. Ball, G. Hancock, F. Winterbottom, Product channels in the near-UV photodissociation of ozone, Faraday Discuss. 100 (1995) 215–227.

[25] C.-H. Wu, C.-L. Chang, C.-Y. Kuo, Decolorization of amaranth by advanced oxidation processes, React. Kinet. Catal. Lett. 86 (2005) 37–43.

[26] J. Zhang, H. Xu, H. Chen, M. Anpo, Study on the formation of H_2O_2 on TiO_2 photocatalysts and their activity for the photocatalytic degradation of X-GL dye, Res. Chem. Intermed. 29 (2003) 839–848.

[27] P.A. Pekakis, N.P. Xekoukoulotakis, D. Mantzavinos, Treatment of textile dyehouse wastewater by TiO_2 photocatalysis, Water Res. 40 (2006) 1276–1286.

[28] M.A. Rauf, S.B. Bukallah, A. Hamadi, A. Sulaiman, F. Hammadi, The effect of operational parameters on the photoinduced decoloration of dyes using a hybrid catalyst V_2O_5/TiO_2, Chem. Eng. J. 129 (2007) 167–172.

[29] A. Aleboyeh, H. Aleboyeh, Y. Moussa, Decolorisation of Acid Blue 74 by ultraviolet/H_2O_2, Environ. Chem. Lett. 1 (2003) 161–164.

[30] C.N.R. Rao, Ultraviolet and Visible Spectroscopy, second ed., Butterworths, London, 1967.

[31] W. Zhao, W. Shi, D. Wang, Ozonation of cationic Red X-GRL in aqueous solution: degradation and mechanism, Chemosphere 57 (2004) 1189–1199.

[32] A. Demirev, V. Nenov, Ozonation of two acidic azo dyes with different substituents, Ozone: Sci. Eng. 27 (2005) 475–485.

[33] A. Loïpez-Loïpez, J.S. Pic, H. Debellefontaine, Ozonation of azo dye in a semi-batch reactor: a determination of the molecular and radical contributions, Chemosphere 66 (2007) 2120–2126.

[34] F.J. Beltran, Ozone Reaction Kinetics for Water and Wastewater System, CRC Press CLL, New York, 2004.